Available online at www.sciencedirect.com
SCIENCE DIRECT®
Journal of Organometallic Chemistry 689 (2004) 2103–2113
Journal of Organometallic Chemistry
www.elsevier.com/locate/jorganchem

Synthesis and characterisation of phosphane-substituted Co_3C clusters having a pendant allyl side-chain

Steven J. Black [a], Christopher P. Morley [a,*], Alun E. Owen [a], Mark R.J. Elsegood [b]

[a] Department of Chemistry, University of Wales Swansea, Singleton Park, Swansea SA2 8PP, UK
[b] Chemistry Department, Loughborough University, Loughborough, Leicestershire LE11 3TU, UK

Received 3 November 2003; accepted 11 March 2004

Abstract

Substituted μ_3-carbido-capped tricobalt carbonyl clusters have been synthesised by reaction of $[Co_3(\mu_3\text{-}C(O)OCH_2CH{=}CH_2)(CO)_9]$ with a range of monodentate and chelating phosphane ligands. The products have been characterised by microanalysis, IR and NMR spectroscopy, mass spectrometry and, in the case of $[Co_3(\mu_3\text{-}CR)(CO)_7(dppe)]$, $[Co_3(\mu_3\text{-}CR)(CO)_7(dppm)]$, $[Co_3(\mu_3\text{-}CR)(CO)_7(PPh_3)_2]$, $[Co_3(\mu_3\text{-}CR)(CO)_7(PMe_3)_2]$ and $[Co_3(\mu_3\text{-}CR)(CO)_6(PEt_3)_3]$ ($R = C(O)OCH_2CH{=}CH_2$), single crystal X-ray diffraction.

Keywords: Clusters; Cobalt; Phosphanes; X-ray crystallography

1. Introduction

Supported metal cluster units, whether as discrete particles or as organised carbonyl/organometallic assemblies, are among the most important classes of catalysts in an industrial sense [1]. The ability of transition metal carbonyl clusters to catalyse a wide variety of reactions has been known for many years [2–4]. More specifically, there are several examples of μ_3-alkylidyne tricobalt carbonyl clusters acting as catalysts [5,6], especially those substituted derivatives with phosphane ligands present [7,8]. However, there are problems associated with the use of late transition metal clusters as catalysts, mainly in the recovery and identification of the catalytically active cluster species [9,10], since clusters often have activity arising through decomposition to a mononuclear species such as $[CoH(CO)_4]$ [11,12]. The problem of decomposition can be overcome by using a capping ligand on the cluster and chelating phosphanes to effectively support the metal atoms within the cluster and thereby prevent core fragmentation. The phosphanes are also useful in allowing electron density "tuning" within the core of the cluster to further enhance and direct reactivity.

To this end we have met with success in developing systematic syntheses of a range of cobalt clusters with both monodentate and chelating phosphane ligands. These compounds all incorporate a capping moiety terminating in an unsaturated organic functionality suitable for linking these clusters to a range of solid supports.

Our starting point has been the work on μ_3-alkylidyne tricobalt clusters done by Seyferth et al. [13] who, some decades ago, reported the action of a 2–3 molar excess of aluminium halide AlX_3 ($X = Cl$, Br, I) on halomethylidyne tricobalt nonacarbonyl complexes $[Co_3(\mu_3\text{-}CX)(CO)_9]$ ($X = Cl$, Br) [14,15]. This reaction resulted in the formation of the acylium haloaluminate salt $[Co_3(\mu_3\text{-}CCO)(CO)_9]^+[AlX_4]^-$ even when the reaction was carried out under an inert atmosphere. In contrast with conventional acylium ions, this cation is indefinitely stable under anhydrous conditions. The haloaluminate salt can react with a range of nucleophiles to produce clusters of the type $[Co_3(\mu_3\text{-}CC(O)Y)(CO)_9]$ with $Y = OR$, OAr, NRR′, SR, R, Ar, H, etc.

* Corresponding author. Tel.: +44-1792-295273; fax: +44-1792-295747.
E-mail address: c.p.morley@swan.ac.uk (C.P. Morley).

0022-328X/$ - see front matter © 2004 Elsevier B.V. All rights reserved.
doi:10.1016/j.jorganchem.2004.03.036

2. Results and discussion

Using a method based on that of Seyferth et al., the cluster, $[Co_3(\mu_3\text{-}CC(O)OCH_2CH{=}CH_2)(CO)_9]$ (**1**), was prepared successfully from $[Co_3(\mu_3\text{-}CCl)(CO)_9]$ [16] and allyl alcohol in high yield (Scheme 1) [14]. Phosphane derivatives **2**–**8** were synthesised by stirring a solution of **1** with the required phosphane at room temperature (Scheme 2).

There seems to be a paucity of examples in the literature of clusters being produced via ambient temperature reaction, with electrochemical or thermal methods being much more commonly utilised [17]. However, no apparent disadvantage was detected using ambient temperature reaction. All the reactions produced an identical colour change from purple to dark green. The products were isolated by column chromatography and further purified by recrystallisation if appropriate. Greatest yields were obtained when stirring was continued for between 4 and 18 h, depending on the phosphane in question.

In most cases, a single product was isolated, corresponding to replacement of two of the carbonyl ligands in **1** by the phosphane. Steric factors may be assumed to play a key role in inhibiting further substitution. It is therefore intriguing that a trisubstituted cluster was obtained as the major product of the reaction with triethylphosphane. At present we have no explanation for this apparent anomaly.

The molecular structure of **2** (Fig. 1) shows that the dppe ligand binds in a bridging mode rather than chelating to a single cobalt atom and that it adopts an equatorial configuration in the solid state. There are several other examples of bidentate phosphane ligands bridging two metal centres in this manner [17–19]. The dppe-bridged Co–Co bond (2.5179(9) Å) is somewhat longer than the other two Co–Co bonds with bond lengths of 2.4706(9) and 2.4801(10) Å (Table 1). This phenomenon has been observed previously in dppm-bridged cobalt clusters, with the bond lengthening believed to be a consequence of the bonding requirements of the bridging ligand [17]. Cobalt-capping carbon bond lengths of 1.939(5), 1.893(5) and 1.881(5) Å (Table 1) clearly show a lengthening of the Co-capping carbon bond opposite the phosphane ligand. This indicates that the μ_3-capping (apical) carbon in **2** "leans" towards the

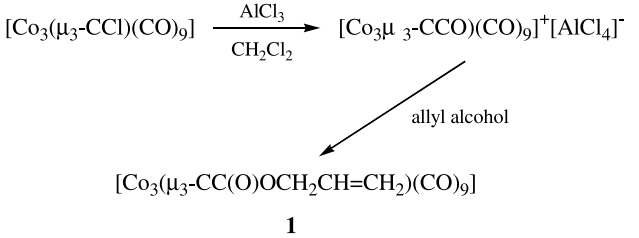

Scheme 1. Preparation of $[Co_3(\mu_3\text{-}CC(O)OCH_2CH{=}CH_2)(CO)_9]$ (**1**).

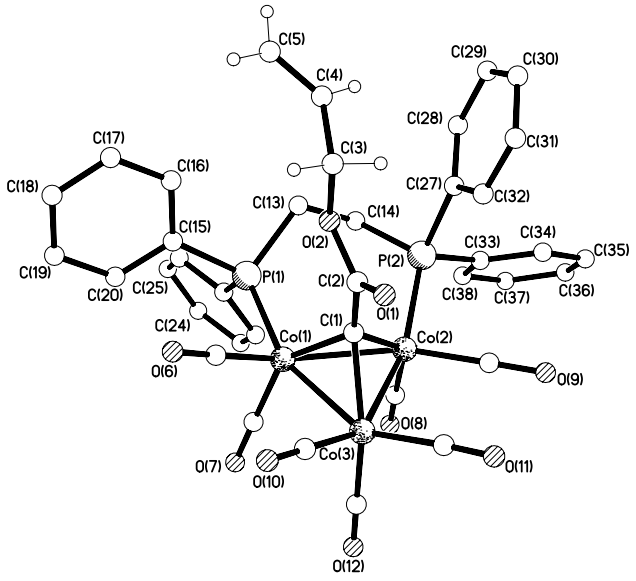

Fig. 1. X-ray crystal structure of $[Co_3(\mu_3\text{-}CC(O)OCH_2\text{-}CH{=}CH_2)(CO)_7(dppe)]$ (**2**).

two cobalt atoms bonded to the phosphane ligand. Downard et al. [17] have described this type of apical carbon as adopting a "semicapping orientation" with respect to the three cobalt atoms. The displacement can be explained in terms of electronic effects. Greater electron density will be localised on the cluster arising from substitution of carbon monoxide with phosphane ligands, the latter's ability as a better σ-donor and worse π-acceptor voluminously documented. However, the equatorially coordinated dppe ligand prevents the adoption of a carbonyl-bridged structure to dissipate the increased electron density on the cluster core. In this case, electron density can be dissipated through the interaction of appropriate π-orbitals of the apical carbon and orbitals of Co(1) and Co(2) [17]. Thus the observed "semicapping orientation" is assumed.

The bond lengths and angles in the capping moiety of **2** are comparable to those in its parent analogue [15], **1**, except for two parameters: the lengthening of the C(1)–C(2) bond from 1.479(5) to 1.506(6) Å, and the elongation of C(3)–C(4) to 1.504(9) Å (cf. 1.471(5) Å). Selected bond lengths and angles of the structure are listed in Tables 1 and 2.

The spectroscopic information suggests that the structure of **2** in solution is identical to that in the solid state. The infrared spectrum of **2** (Table 3) contains five bands corresponding to terminal carbonyl absorptions, with no evidence for the existence of an isomer containing bridging carbonyls. Mass spectrometry (Table 3), in addition to confirming the molecular ion, shows sequential loss of carbonyl ligands. This is a characteristic feature in the mass spectra of carbonyl clusters and is observed for all the clusters described herein. The NMR data (Tables 4–6) are as expected.

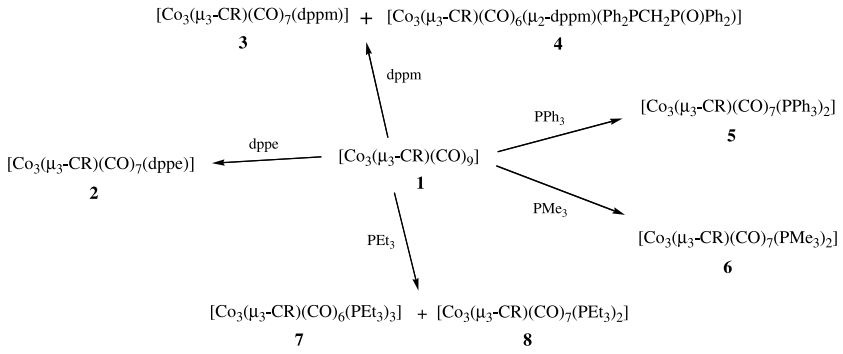

Scheme 2. Products obtained from the reactions of **1** with phosphanes (R = C(O)OCH$_2$CH=CH$_2$).

Table 1
Selected bond lengths (Å) for **2**, **3**, **5**, **6** and **7**

	2	**3**	**5**[a]	**5′**[a]	**6**	**7**
Co(1)–Co(2)	2.5179(9)	2.5030(4)	2.4975(12)	2.4962(10)	2.4834(3)	2.418(2)
Co(2)–Co(3)	2.4801(10)	2.4814(4)	2.4854(11)	2.4953(10)	2.4782(3)	2.486(2)
Co(1)–Co(3)	2.4706(9)	2.4712(4)	2.4953(11)	2.5061(10)	2.4947(3)	2.491(3)
Co(1)–C(1)	1.893(5)	1.8902(18)	1.942(7)	1.892(5)	1.8914(17)	1.904(13)
Co(2)–C(1)	1.881(5)	1.8936(18)	1.839(7)	1.918(5)	1.8904(17)	1.898(14)
Co(3)–C(1)	1.939(5)	1.9323(17)	1.907(6)	1.895(5)	1.9102(17)	1.968(13)
C(1)–C(2)	1.506(6)	1.478(3)	1.472(9)	1.486(7)	1.472(2)	1.463(18)
C(2)–O(1)	1.201(6)	1.211(2)	1.172(9)	1.201(6)	1.217(2)	1.217(17)
C(2)–O(2)	1.328(6)	1.354(2)	1.359(12)	1.353(7)	1.347(2)	1.298(19)
O(2)–C(3)	1.452(6)	1.454(3)	1.514(14)	1.453(6)	1.451(2)	1.437(19)
C(3)–C(4)	1.504(9)	1.478(4)	1.529(19)	1.507(12)	1.479(3)	1.33(3)
C(4)–C(5)	1.301(10)	1.311(4)	1.12(2)	1.129(16)	1.279(3)	1.34(3)
Co(1)–P(1)	2.2130(14)	2.2023(5)	2.2504(16)	2.2403(16)	2.2096(5)	2.198(4)
Co(2)–P(2)	2.2037(14)	2.2198(5)	2.2381(18)	2.2456(14)	2.2208(6)	2.211(4)
Co(3)–P(3)	–	–	–	–	–	2.259(4)

[a] **5** and **5′** refer to the two cobalt clusters in the asymmetric unit.

Table 2
Selected bond angles (°) for **2**, **3**, **5**, **6** and **7**

	2	**3**	**5**[a]	**5′**[a]	**6**	**7**
Co(1)–Co(2)–Co(3)	59.24(3)	59.442(12)	60.10(3)	60.27(3)	60.371(9)	61.05(7)
Co(2)–Co(1)–Co(3)	59.61(3)	59.844(11)	59.71(3)	59.85(3)	59.712(9)	60.83(7)
Co(2)–Co(3)–Co(1)	61.14(3)	60.715(10)	60.19(3)	59.88(3)	59.917(9)	58.12(7)
Co(1)–C(1)–Co(2)	83.71(18)	82.83(7)	82.6(3)	81.87(19)	82.09(6)	79.0(5)
Co(1)–C(1)–Co(3)	80.29(19)	80.55(7)	80.8(2)	82.9(2)	82.02(7)	80.1(5)
Co(2)–C(1)–Co(3)	80.94(18)	80.86(7)	83.1(3)	81.75(19)	81.39(7)	80.0(5)
Co(1)–C(1)–C(2)	131.8(4)	132.01(13)	129.7(7)	134.9(4)	128.95(13)	131.5(10)
Co(2)–C(1)–C(2)	135.7(4)	131.31(13)	132.9(6)	128.8(4)	131.64(12)	132.6(11)
Co(3)–C(1)–C(2)	124.4(3)	130.01(13)	129.1(6)	127.9(4)	131.97(12)	132.7(11)
C(1)–C(2)–O(1)	123.9(5)	125.16(18)	129.7(8)	126.2(5)	125.41(17)	119.9(14)
O(1)–C(2)–O(2)	123.9(5)	122.04(17)	119.6(7)	122.2(5)	121.83(17)	120.8(13)
C(1)–C(2)–O(2)	112.3(4)	112.80(16)	110.3(7)	111.6(4)	112.76(14)	119.2(12)
C(2)–O(2)–C(3)	115.5(4)	117.19(17)	114.6(10)	116.9(5)	115.00(14)	118.6(13)
O(2)–C(3)–C(4)	107.3(5)	112.9(2)	100.1(13)	105.6(6)	109.05(16)	116(2)
C(3)–C(4)–C(5)	124.5(7)	127.2(2)	120(3)	131.8(15)	127.4(2)	131(2)
C(1)–Co(1)–P(1)	110.56(15)	104.10(5)	119.65(18)	126.84(16)	105.55(5)	100.8(4)
C(1)–Co(2)–P(2)	106.47(15)	104.07(5)	119.5(2)	113.14(15)	97.92(5)	102.7(4)
C(1)–Co(3)–P(3)	–	–	–	–	–	162.8(4)

[a] **5** and **5′** refer to the two cobalt clusters in the asymmetric unit.

Table 3
Infrared and FAB mass spectrometry data

Compound	ν(CO)[a]	Mass spectrometry[b]
2	2065 (s), 2014 (s), 2010 (vs), 1998 (m), 1978 (w)	868 [M^+]
3	2067 (m), 2016(vs, br), 1975(sh)	877 [M^+ + Na], 855 [M^+ + H]
4	2029 (m), 1994 (s), 1976 (s), 1944 (sh)	1170 [M^+ – 2CO]
5	2083 (w), 2055 (vs), 2029 (w), 1999 (w), 1970 (m)	995 [M^+ + H]
6	2053 (s), 2000 (vs), 1962 (sh), 1950 (w), 1911 (w)	645 [M^+ + Na], 623 [M^+ + H], 622 [M^+]
7	2050 (m), 1998 (s), 1977 (vs), 1806 (m), 1740 (w), 1700 (vw)	796 [M^+]
8	2062 (m), 2012 (vs), 1994 (s), 1981 (w), 1975 (vw)	729 [M^+ + Na], 707 [M^+ + H]

[a] Absorption maxima in cm^{-1}. Abbreviations used: vs, very strong; s, strong; m, medium; w, weak; vw, very weak and sh, shoulder.
[b] m/z values and assignments of molecular ion peaks. All compounds also exhibited fragment ion peaks due to sequential loss of carbonyl ligands.

Table 4
^{1}H NMR data[a]

	2	**3**	**4**	**5**	**6**	**7**	**8**
CH_3	–	–	–	–	1.42–1.46[e]	0.8–1.2	0.92–1.14
CH_2	1.94–2.34	3.30–3.45[d] 4.39–4.54[d]	3.30–3.45[d] 4.11–4.26[d] 3.25–3.65	–	–	1.5–1.9	1.61–1.83
H_d[b]	3.98–4.11	4.49–4.59	3.99–4.09	4.31–4.48	4.57–4.60	4.6–4.7	4.49–4.62
H_b[b,c]	4.85–4.95	5.03–5.11	4.85–4.98	4.95–5.05	5.17–5.21	5.0–5.2	5.06–5.18
H_c[b,c]	5.05–5.10	5.17–5.26	5.02–5.07	5.15–5.32	5.29–5.38	5.27–5.41	5.23–5.34
H_a[b,c]	5.53–5.76	5.70–5.84	5.48–5.60	5.72–5.96	5.87–6.01	5.73–5.98	5.83–5.97
Ph	7.02–7.69	6.95–7.44	6.93–7.74	7.10–7.64	–	–	–

[a] Chemical shifts (δ) in ppm.
[b] For key to assignments see Fig. 7.
[c] For all compounds: $J(H_b–H_a) = 10.8$ Hz; $J(H_c–H_a) = 18.3$ Hz.
[d] $^2J(^1H–^{31}P) \sim J(^1H–^1H) \sim 14.6$Hz.
[e] $J(^1H–^{31}P) = 9.2$ Hz.

Table 5
^{13}C NMR data[a]

	2	**3**	**4**	**5**	**6**	**7**	**8**
P*C*H_3	–	–	–	–	19.7[h]	8.1	6.8
P*C*H_2	23.4[c]	39.7[f]	32.4, 38.1[g]	–	–	18.8[i], 20.9[j]	19.5[j]
C_3[b]	64.5	64.6	64.6	66.0	66.0	66.0	64.6
C_5[b]	116.2	116.1	116.1	117.3	118.3	117.4	116.5
C_4[b]	N.O.[d,e]	N.O.[d,e]	N.O.[d,e]	N.O.[d,e]	133.3	132.3	132.1
Ph	127.4–136.6	126.9–136.1	126.4–137.1	128.5–135.0	–	–	–
C_1[b]	181.3	182.7	183.6	N.O.[d]	N.O.[d]	N.O.[d]	181.1
CO	205.0	N.O.[d]	N.O.[d]	205.4	N.O.[d]	N.O.[d]	207.8

[a] Chemical shifts (δ) in ppm.
[b] For key to assignments see Fig. 7.
[c] $^1J(^{13}C–^{31}P) = 26.0$ Hz.
[d] N.O. = Not observed.
[e] Signal obscured by phenyl resonances.
[f] $^1J(^{13}C–^{31}P) = 23.1$ Hz.
[g] $^1J(^{13}C–^{31}P) = 22.2$ Hz.
[h] $^1J(^{13}C–^{31}P) = 27.7$ Hz.
[i] $^1J(^{13}C–^{31}P) = 22.1$ Hz.
[j] $^1J(^{13}C–^{31}P) = 23.3$ Hz.

The structure of **3** (Fig. 2), a dppm-bridged product, has much in common with the dppe-bridged product discussed above. Selected bond lengths and angles are listed in Tables 1 and 2. The Co–Co bond bridged by the dppm is lengthened (2.5030(4) Å), although to a lesser extent than in **2**, compared to the other two Co–Co bonds (ave. 2.4763(4) Å). The alkylidyne carbon also exhibits the expected "semicapping orientation," leaning towards the phosphane bridged Co–Co bond despite the steric congestion. Each phosphorus atom of the dppm

Table 6
^{31}P NMR data

Compound	2	3	4	5	6	7	8
δ (ppm)	47.3	33.3	22.1[a] 32.9[b] 37.9	45.4	2.9	33.2	33.7

[a] $^2J(^{31}P–^{31}P) = 31$ Hz.
[b] $^3J(^{31}P–^{31}P) = 43$ Hz.

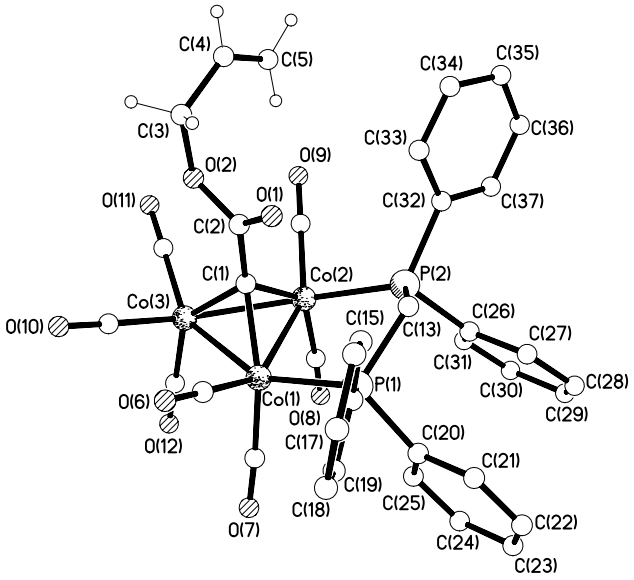

Fig. 2. X-ray crystal structure of $[Co_3(\mu_3\text{-}CC(O)OCH_2CH{=}CH_2)(CO)_7(dppm)]$ (**3**).

ligand binds equatorially to a cobalt atom, thus bridging a Co–Co bond, forming a thermodynamically stable five-membered ring. The ring takes the form of a boat conformation, which is not surprising given the fact that the same conformation has been reported for other dppm-bridged Co_3C clusters [20,21].

The spectroscopic information recorded (Tables 3–6) is in line with expectation and indicates that **3** adopts the same structure in the solid and solution states. More peaks would have been expected in the carbonyl region of the infrared spectrum. However, the broad peak at 2016 cm^{-1} may obscure some of the weak peaks. The ^{1}H NMR spectrum clearly shows the inequivalence of the methylene protons on the dppm ligand. The apparent quartets at 3.38 and 4.44 ppm are presumably doublets of triplets and each corresponds to one of the two hydrogen atoms. The observed pattern of lines arises from the similiarity of the coupling constants, $^2J(^{31}P–^1H)$ and $^2J(^1H–^1H)$ (ca. 14.6 Hz). Remaining signals in the ^{1}H NMR spectrum show good agreement with those expected of the capping moiety. Not all of the expected signals are, however, present in the ^{13}C NMR spectrum. Those for the apical carbon, and the carbonyl carbon to which it is bound, are not observed. This is the case with the ^{13}C NMR spectra recorded for many of the new compounds reported here. The ^{31}P NMR spectrum contains a single resonance at 33.3 ppm, indicating that the two phosphorus atoms of dppm are equivalent.

After the isolation of **3**, a further three bands were eluted from the column, which were either pale brown or pale green. Evaporation of the solvent under reduced pressure in each case yielded only traces of material. Finally, a dark green band was eluted. After solvent removal, again under reduced pressure, a dark green oily residue was isolated, which had a ^{31}P NMR spectrum containing six resonances, at 37.9 (br), 32.9 (br), 29.3 (d), 25.0, 22.1 (d) and −28.4 (d) ppm. The doublets at 29.3 and −28.4 ppm with $J(^{31}P–^{31}P) \sim 50$ Hz may be assigned to the presence of dppm monoxide, $Ph_2PCH_2P(O)Ph_2$ [22]. Traces of dppm dioxide, $Ph_2P(O)CH_2P(O)Ph_2$, are revealed by the peak at 25.0 ppm [23].

Dissolving the dark green oily solid in dichloromethane and adding hexane precipitated **4**, the compound responsible for the other three resonances in the ^{31}P NMR spectrum. Attempts to crystallise **4** under a variety of conditions were unsuccessful, but on the basis of mass spectrometry, NMR and infrared spectroscopy (Tables 3–6) it has been characterised as $[Co_3(\mu_3\text{-}CC(O)OCH_2CH{=}CH_2)(CO)_6(\mu_2\text{-dppm})(Ph_2PCH_2P(O)Ph_2)]$.

The mass spectrum of **4** supports the postulate that a higher mass cluster, i.e., more highly substituted than **3**, has been produced. Although it does not contain a peak corresponding to $[M^+]$, one corresponding to $[M^+ - 2CO]$ is observed. The ^{31}P resonance at 32.9 ppm may be assigned to a dppm-ligand bridging two cobalt atoms, by substituting two equatorial carbonyls, as in **3**. All the carbonyl ligands must be terminally bonded, as they are precluded from adopting a bridging configuration by the bridging phosphane ligand. The absence of bridging carbonyls was confirmed by the infrared spectrum. The ^{31}P NMR signals at 37.9 and 22.1 ppm are in the range expected for a coordinated phosphane and a phosphoryl group, $Ph_2P{=}O$, respectively, implying that a dppm monoxide ligand is present, acting as a monodentate ligand via the phosphorus(III) atom. This supposition is supported by the observation in the infrared spectrum of **4** of a very strong absorption at 1270 cm^{-1} which is in the range reported for the P=O group.

It may be presumed that **4** is formed by oxidation of an intermediate of the form $[Co_3(\mu_3\text{-}CC(O)OCH_2\text{-}CH{=}CH_2)(CO)_6(\mu_2\text{-dppm})(dppm)]$, although spectroscopic evidence for the existence of this species remains elusive. Compound **4** can, however, be prepared by treatment of **3** with further dppm and subsequent column chromatography. Other structures have been reported where the pendant or dangling phosphorus centre has been oxidised [24,25].

Monosubstituted triphenylphosphane derivatives of Co_3C clusters are well known [5,14,26–28] but examples of disubstituted derivatives are much rarer [26,29,30]. A disubstituted derivative, **5** (Fig. 3), resulted from reaction at ambient temperature. The crystal structure of **5** has been determined as the hexane/dichloromethane solvate. The asymmetric unit comprises two cobalt clusters, plus the incorporation of half each of a molecule of hexane and dichloromethane. Thus a quarter of dichloromethane and a quarter of hexane are incorporated per cluster. The two clusters differ mainly in the conformation of the capping moiety (see Tables 1 and 2). In the cluster labelled Co(1), Co(2), etc. the capping ligand leans towards the Co(1)–Co(2) bond, as evidenced by the bond angles C(2)–C(1)–Co, while in that containing Co(4), Co(5), Co(6), etc. the capping fragment lies above Co(4).

Perhaps the most surprising feature of the structure of **5** is that all the carbonyl ligands are terminally bonded. Analysis of the infrared spectrum (Table 3) also indicates the absence of bridging carbonyl ligands in solution. This is rather unexpected since disubstitution of Co_3C clusters by poor π-accepting, bulky phosphane ligands very often results in carbonyl-bridged structures with displacement of the axial carbonyl ligands. Bridging carbonyl ligands would offer steric relief and reduce the electron density localised on the Co_3C core through more effective dπ(Co)–π*(CO) back donation. Indeed, Robinson et al. reported that for complexes of general formula $[Co_3(\mu_3\text{-}CY)(CO)_7L_2]$, where Y = Me, Ph or F and L = PPh_3, PBu_3, $PPhEt_2$ etc., a carbonyl-bridged structure was exclusively adopted [29].

This structure also shows that the phosphane ligands have substituted at equatorial positions. As pointed out previously, this is most likely to arise because of steric effects. The bulky triphenylphosphane ligands have only one neighbouring equatorial carbonyl ligand on an adjacent cobalt atom. If coordinated axially the phosphane ligand would have two axially coordinated carbonyls nearby. The ^{31}P NMR spectrum (Table 6) contains a single resonance at $\delta = 45.4$ ppm and thus indicates that the phosphane ligands are equivalent.

The C(1)–Co(1)–P(1) and C(1)–Co(2)–P(2) angles (Table 2) of 119.65(18)° and 119.5(2)° are relatively large compared to that reported for the monosubstituted derivative (96.0(5)°) [28]. This bending of the Co–P bonds towards the tricobalt plane reflects the intramolecular repulsive non-bonded interaction between the phenyl rings of the phosphane ligands and the capping moiety.

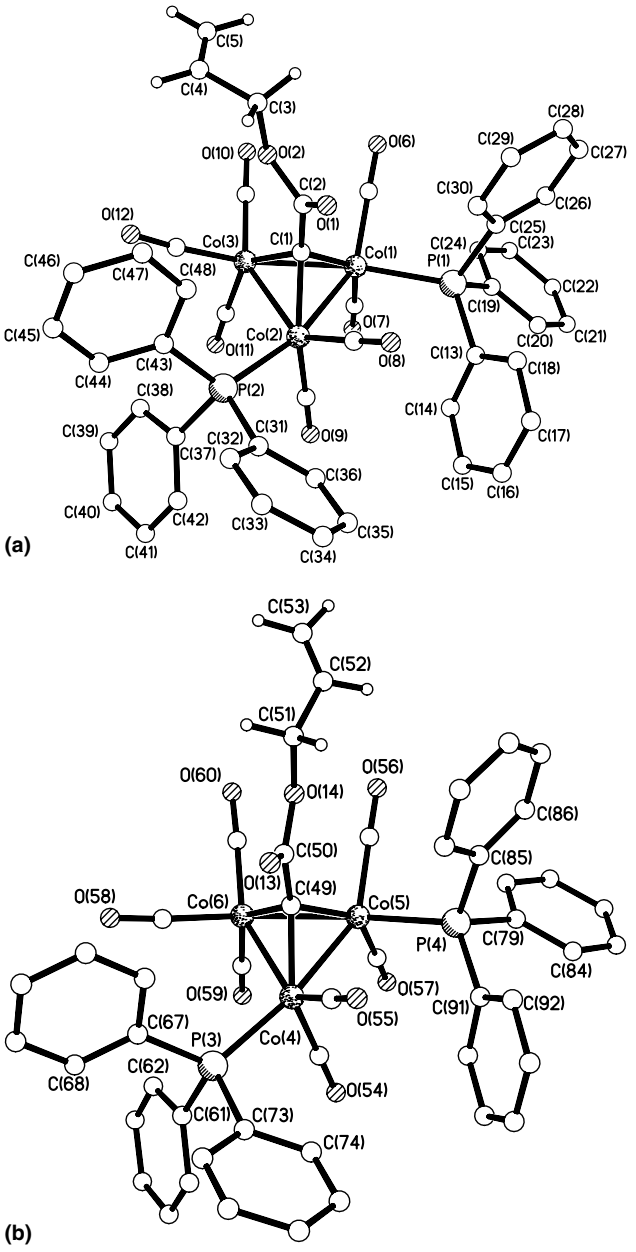

Fig. 3. X-ray crystal structure of $[Co_3(\mu_3\text{-}CC(O)OCH_2CH{=}CH_2)(CO)_7(PPh_3)_2]$ (**5**), showing the two cobalt clusters that comprise the asymmetric unit.

The derivative produced from the reaction with trimethylphosphane, **6**, is also a disubstituted cluster and the cluster's preference for equatorial substitution is again shown by the replacement of two equatorial carbonyl ligands with phosphane ligands (Fig. 4). The bond lengths and angles in the cluster core and capping moiety generally conform closely to those in $[Co_3(\mu_3\text{-}CC(O)OCH_2CH{=}CH_2)(CO)_9]$ [15] with few exceptions. The three Co–Co bond lengths (Table 1) all exhibit a very small lengthening compared to that observed in the

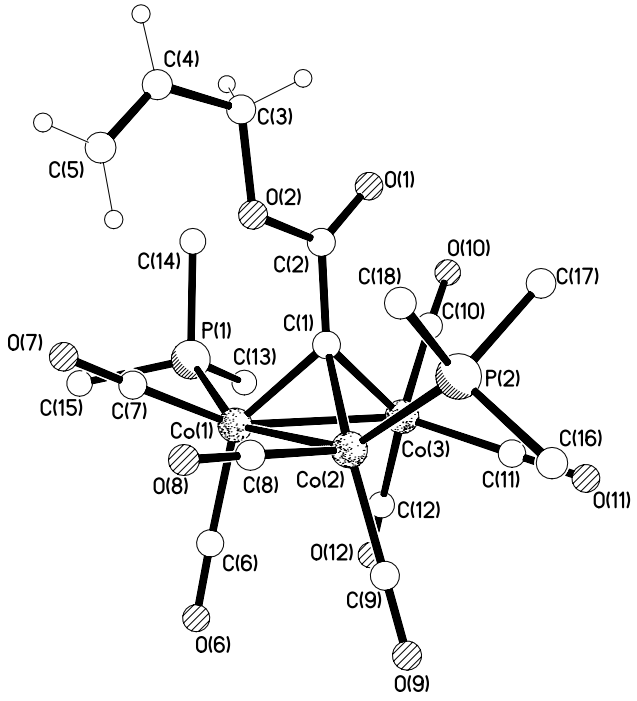

Fig. 4. X-ray crystal structure of $[Co_3(\mu_3\text{-}CC(O)OCH_2CH{=}CH_2)(CO)_7(PMe_3)_2]$ (**6**).

parent structure, as do all the other structures reported herein, as anticipated. Also, the C(4)–C(5) bond length of 1.279(3) Å is noted to be considerably shortened (cf. 1.305(6) Å) [15].

Trimethylphosphane is the least sterically bulky ligand used for ligand substitution in the experiments reported here. This is reflected in the C(1)–Co–P bond angles (Table 2). Angles of 105.55(5)° and 97.92(5)° have been determined for C(1)–Co(1)–P(1) and C(1)–Co(2)–P(2), respectively. These are considerably less than the comparable angles determined for the other structures reported herein. Non-bonded interactions between the phosphane ligands and the capping moiety are reduced as a consequence of the relatively small size of the trimethylphosphane ligand. For comparison, an average C(1)–Co–P bond angle of 111° was reported by Simpson and coworkers [31] for the cluster $[Co_3(\mu_3\text{-}CCH_3)(CO)_6(P(OMe)_3)_3]$.

The average C(1)–Co–P bond angle, determined for each disubstituted cluster derivative, was plotted against the cone angle, as reported by Tolman [34], of the phosphane ligand in question. The data points share an approximately linear relationship, as shown in Fig. 5. Thus it is clearly observed that the steric properties of the phosphane ligand influence the degree to which the Co–P bond is bent away from or towards the tricobalt plane.

When green crystals were isolated from the reaction of **1** with 1.61 equivalents of triethylphosphane, it was assumed that a disubstituted cluster had again been produced. The FAB mass spectrum, however, indicated that the product was in fact the trisubstituted cluster. An X-ray diffraction study of **7** proved this to be the case (Fig. 6). The reason for the production of a trisubstituted cluster has not yet been established. However, the reaction with triethylphosphane was more vigorous than those with the other phosphane ligands (N.B. trimethylphosphane was added as the silver iodide adduct). The reaction produced rapid effervescence, assumed to be carbon monoxide, which ceased after two hours when it was assumed that the reaction had proceeded to completion.

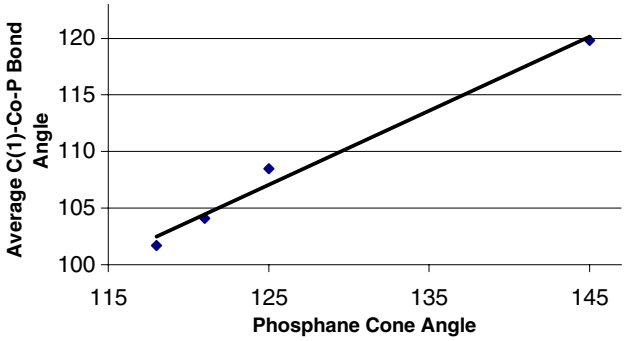

Fig. 5. Graph of phosphane cone angle versus average C(1)–Co–P bond angle in structures of **2**, **3**, **5** and **6**.

The high *R* values, twinning, and disorder in the crystal structure of **7** (Table 7) mean that discussion of

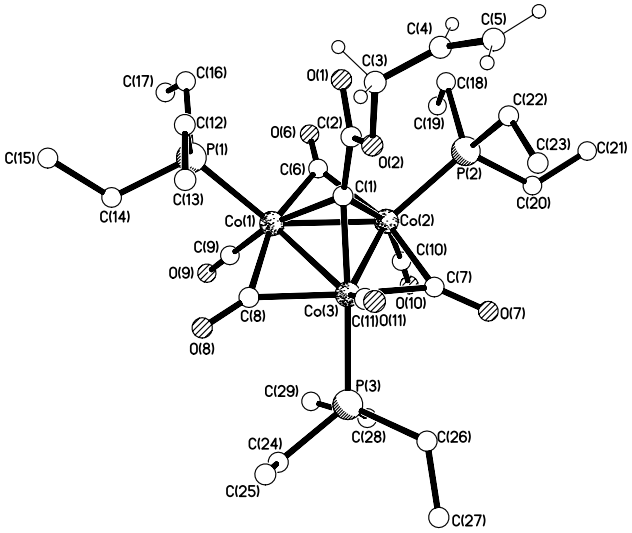

Fig. 6. X-ray crystal structure of $[Co_3(\mu_3\text{-}CC(O)OCH_2CH{=}CH_2)(CO)_6(PEt_3)_3]$ (**7**).

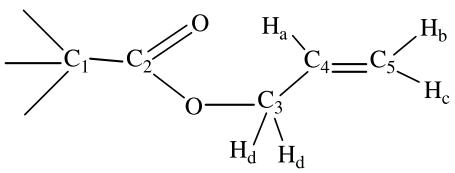

Fig. 7. Key to NMR assignments for capping group.

Table 7
Crystal data and structure refinement for **2**, **3**, **5**, **6** and **7**

	2	**3**	**5**	**6**	**7**
Chemical formula	$C_{38}H_{29}Co_3O_9P_2$	$C_{40}H_{34}Co_3O_9P_2$	$C_{49.75}H_{39}Cl_{0.5}Co_3O_9P_2$	$C_{18}H_{23}Co_3O_9P_2$	$C_{29}H_{50}Co_3O_8P_3$
Formula weight	868.34	897.40	1037.26	622.09	796.39
Crystal system	Orthorhombic	Monoclinic	Triclinic	Orthorhombic	Orthorhombic
Space group	$P2_12_12_1$	$P2_1/n$	$P\bar{1}$	$P2_12_12_1$	$P2_12_12_1$
Unit cell lengths	$a = 13.2057(9)$ Å $b = 14.2109(9)$ Å $c = 19.7833(13)$ Å	$a = 14.8285(17)$ Å $b = 15.6559(18)$ Å $c = 16.8160(19)$ Å	$a = 11.3011(11)$ Å $b = 20.749(2)$ Å $c = 21.897(2)$ Å	$a = 10.2499(6)$ Å $b = 12.7164(7)$ Å $c = 19.2840(11)$ Å	$a = 19.5908(7)$ Å $b = 10.7239(4)$ Å $c = 17.2704(6)$ Å
Unit cell angles	$\alpha = 90°$, $\beta = 90°$, $\gamma = 90°$	$\alpha = 90°$, $\beta = 92.301(2)°$, $\gamma = 90°$	$\alpha = 114.365(2)°$, $\beta = 91.815(2)°$, $\gamma = 101.376(2)°$	$\alpha = 90°$, $\beta = 90°$, $\gamma = 90°$	$\alpha = 90°$, $\beta = 90°$, $\gamma = 90°$
Cell volume	3712.6(4) Å^3	3900.7(8) Å^3	4548.6(8) Å^3	2513.5(2) Å^3	3628.3(2) Å^3
Z	4	4	4	4	4
Absorption coefficient μ	1.465 mm^{-1}	1.397 mm^{-1}	1.238 mm^{-1}	2.127 mm^{-1}	1.531 mm^{-1}
Crystal colour and size	Red, $0.32 \times 0.26 \times 0.22$ mm^3	Dark green, $0.93 \times 0.77 \times 0.45$ mm^3	Brown, $0.49 \times 0.39 \times 0.31$ mm^3	Dark green, $0.20 \times 0.17 \times 0.17$ mm^3	Red, $0.28 \times 0.24 \times 0.15$ mm^3
Reflections collected	29,767	32,510	36,042	21,907	19,552
Independent reflections	8417 ($R_{int} = 0.0437$)	9231 ($R_{int} = 0.0327$)	19,578 ($R_{int} = 0.0365$)	6043 ($R_{int} = 0.0271$)	6377 ($R_{int} = 0.0224$)
Reflections with $F^2 > 2\sigma(F^2)$	7375	7128	13,067	5652	6291
Final R indices $[F^2 > 2\sigma(F^2)]$	$R_1 = 0.0655$, $wR_2 = 0.1526$	$R_1 = 0.0289$, $wR_2 = 0.0673$	$R_1 = 0.0679$, $wR_2 = 0.1638$	$R_1 = 0.0208$, $wR_2 = 0.0460$	$R_1 = 0.0954$, $wR_2 = 0.2363$
R indices (all data)	$R_1 = 0.0756$, $wR_2 = 0.1663$	$R_1 = 0.0431$, $wR_2 = 0.0715$	$R_1 = 0.1062$, $wR_2 = 0.1904$	$R_1 = 0.0240$, $wR_2 = 0.0473$	$R_1 = 0.0966$, $wR_2 = 0.2370$

bond lengths and angles is inappropriate. The connectivity is, however, assured. It is noted that two of the phosphane ligands are equatorially bound whilst the other is axially coordinated. The fact that only one resonance is observed in the ^{31}P NMR spectrum indicates that the phosphorus nuclei are equivalent on the timescale of the NMR experiment. This could be achieved via one of two mechanisms: exchange of bridging and terminal carbonyl ligands similar to that observed in $[Rh_4(CO)_{12}]$ [32], or interconversion of axial/equatorial ligands [33]. It is notable also that the ^{1}H and ^{13}C NMR spectra of **7** are generally broad and weak, as would be characteristic of a fluxional system at intermediate temperatures.

A second band was obtained from this reaction via column chromatography, which was an identical colour to the first. Spectroscopic analysis of the resultant solid indicated that a disubstituted derivative, **8**, had been produced. Attempts at crystallising this product, from a variety of solvents and at low temperatures, failed and thus no X-ray data can be presented.

The ^{1}H and ^{13}C NMR spectra of **8** are as expected (Tables 4 and 5). A single resonance is observed in the ^{31}P NMR spectrum (Table 6), with a small difference in chemical shift between compounds **7** and **8** (33.2 and 33.7 ppm, respectively). Mass spectrum data support the proposition that the second fraction is indeed the disubstituted triethylphosphane derivative. This still leaves the question as to the orientation of the ligands around the cluster core in **8**. The infrared data are consistent with those of **5** and **6** (Table 3) and thus an analogous structure, in which triethylphosphane ligands have substituted two equatorial carbonyl ligands with all remaining carbonyl ligands in a terminal configuration, is proposed.

3. Conclusion

A range of tricobalt clusters has been synthesised and characterised, containing both monodentate and bidentate phosphane ligands, with an unsaturated allyl capping moiety. We shall shortly report on the synthesis of a corresponding series of derivatives possessing a longer acryl capping group. The utility of these derivatives as hydroformylation catalysts will also be discussed.

4. Experimental

All reactions were carried out under an argon or dinitrogen atmosphere using standard Schlenk methodology. All solvents were dried by boiling for at least 5 h with either Na/K alloy, or, in the case of halogenated solvents, CaH_2, before being distilled under an atmosphere of dinitrogen. Mass spectra were recorded at the EPSRC Mass Spectrometry Service Centre using Fast

Atom Bombardment (FAB). ^{1}H and ^{13}C NMR spectra were obtained at 400.14 and 100.61 MHz, respectively, on a Bruker AC400 spectrometer using tetramethylsilane as an internal standard. ^{31}P NMR spectra were obtained at 101.26 MHz using a Bruker WM250 spectrometer with 85% phosphoric acid as an external standard. IR spectra were recorded in solution using a Mattson Satellite FTIR spectrometer. Melting points were recorded in sealed capillaries under dinitrogen and are uncorrected. Elemental analyses were carried out by the analytical service, University of Wales Cardiff, or at Butterworth Laboratories Ltd. X-ray crystallography studies were carried out at Loughborough University.

$[Co_3(\mu_3\text{-}CCl)(CO)_9]$ [16] and $[Co_3(\mu_3\text{-}CC(O)OCH_2\text{-}CH{=}CH_2)(CO)_9]$ (**1**) [14] were prepared according to the literature methods. Triphenylphosphane was obtained from Aldrich and purified by recrystallisation from warm ethanol to remove traces of Ph_3PO. Dppe was obtained from Strem and was used without further purification. The other phosphane ligands utilised, dppm, trimethylphosphane silver iodide adduct and triethylphosphane, were obtained from Aldrich. $AlCl_3$ was purified by sublimation at 100 °C and 0.05 mm Hg pressure.

4.1. Syntheses of phosphane-substituted clusters

4.1.1. $[Co_3(\mu_3\text{-}CC(O)OCH_2CH{=}CH_2)(CO)_7(dppe)]$ (2)

$[Co_3(\mu_3\text{-}CC(O)OCH_2CH{=}CH_2)(CO)_9]$ (**1**) (0.39 g, 0.74 mmol), dichloromethane (15 mL) and dppe (0.30 g, 0.74 mmol) were stirred for 18 h at room temperature. The reaction was accompanied by a colour change from purple to dark green. TLC was used to show only one species present in solution. The solvent was removed in vacuo and the residue chromatographed on silica using a 70:30 hexane/dichloromethane mixture as eluent. Concentration of the dark green band, followed by cooling to −10 °C resulted in crystallisation of **2**. Yield: 0.14 g, 22%. m.p.: 102–105 °C. $C_{38}H_{29}Co_3P_2O_9$: calcd. C 52.56, H 3.37; found C 51.20, H 3.75. ^{1}H NMR: $\delta = 1.94$ - 2.34 (m, 4H), 3.98–4.11 (m, 2H), 4.85–4.95 (m, 1H), 5.05–5.10 (m, 1H), 5.53–5.76 (m, 1H), 7.02–7.69 (m, 20H). ^{13}C NMR: $\delta = 23.4$ (d), 64.5, 116.2, 127.4–136.6, 181.3, 205.0. ^{31}P NMR: $\delta = 47.3$ (br). IR (CH_2Cl_2): $\nu(CO) = 2065$ (s), 2014 (s), 2010 (vs), 1998 (m), 1978 (w) cm^{-1}. MS: m/z 868 [M^+] plus ions corresponding to sequential loss of carbonyl ligands.

4.1.2. $[Co_3(\mu_3\text{-}CC(O)OCH_2CH{=}CH_2)(CO)_7(dppm)]$ (3) and $[Co_3(\mu_3\text{-}CC(O)OCH_2CH{=}CH_2)(CO)_6(dppm)\text{-}(Ph_2PCH_2P(O)Ph_2)]$ (4)

To a solution of **1** (0.38 g, 0.72 mmol) and dichloromethane (15 mL), one equivalent of dppm (0.28 g, 0.72 mmol) was added. Stirring was continued overnight, resulting in a colour change from purple to dark green. The reaction mixture was concentrated and chromatographed on silica with a mixture of hexane/acetone (20:1) as eluent. An initial brown fraction was collected which gave an unidentified product (<10 mg). A second, dark green fraction was collected which, after concentration to approximately 10 mL and slow cooling to −10 °C overnight, yielded **3**. Yield: 0.19 g, 31%. m.p.: 160–161 °C. ^{1}H NMR: $\delta = 3.30$ - 3.45 (dt, 1H), 4.39–4.54 (dt, 1H), 4.49–4.59 (m, 2H), 5.03–5.11 (m, 1H), 5.17–5.26 (m, 1H), 5.70–5.84 (m, 1H), 6.95–7.44 (m, 20H). ^{13}C NMR: $\delta = 39.7$ (t), 64.6, 116.1, 126.9–136.1, 182.7. ^{31}P NMR: $\delta = 33.3$ (br). IR (CH_2Cl_2): $\nu(CO) = 2067$ (m), 2016 (vs, br), 1975 (sh) cm^{-1}. MS: m/z 877 [$M^+ + Na$], 855 [$M^+ + H$] plus ions corresponding to sequential loss of carbonyl ligands.

Further elution yielded bands which were pale green, pale brown and dark green. Evaporation of the solvent under reduced pressure in the last case resulted in the isolation of **4** as an oily solid, $[Co_3(\mu_3\text{-}CC(O)OCH_2\text{-}CH{=}CH_2)(CO)_6(dppm)(Ph_2PCH_2P(O)Ph_2)]$. This was purified by dissolution in a small volume of dichloromethane, and re-precipitation by addition of hexane. Yield: 0.05 g, 9%. ^{1}H NMR: $\delta = 3.30$ - 3.55 (m, 3H), 3.99–4.27 (m, 3H), 4.85–4.98 (m, 1H), 5.02–5.07 (m, 1H), 5.48–5.60 (m, 1H), 6.93–7.74 (m, 40H). ^{13}C NMR: $\delta = 32.4$ (m), 38.1 (t), 64.6, 116.1, 126.4–137.1, 183.6. ^{31}P NMR: $\delta = 22.1$(d), 32.9 (br, d), 37.9 (br, m). IR (CH_2Cl_2): $\nu = 2029$ (m), 1994 (s), 1976 (s), 1944 (sh), 1423 (s), 1270 (vs) cm^{-1}. MS: m/z 1170 [$M^+ - 2CO$] plus ions corresponding to sequential loss of carbonyl ligands.

4.1.3. $[Co_3(\mu_3\text{-}CC(O)OCH_2CH{=}CH_2)(CO)_7(PPh_3)_2]$ (5)

A solution of **1** (0.22 g, 0.42 mmol), dichloromethane (15 mL) and PPh_3 (0.22 g, 0.84 mmol) was stirred at ambient temperature overnight, during which time a colour change from purple to dark green was observed. After the solvent was removed in vacuo the residue was dissolved in a minimal volume of hexane and chromatographed on alumina. Elution with hexane resulted in a purple fraction being collected containing starting material **1**. Further elution using dichloromethane afforded a dark green band. The dichloromethane was removed by evaporation under reduced pressure and the residue dissolved in hexane/dichloromethane (9:1). Cooling overnight yielded the crystalline product. Yield: 0.07 g, 17%. m.p.: 132 °C dec. $C_{48}H_{35}Co_3O_9P_2$: calcd. C 57.97, H 3.55; found C 57.93, H 4.00. ^{1}H NMR: $\delta = 4.31$ - 4.48 (m, 2H), 4.95–5.05 (m, 1H), 5.15–5.32 (m, 1H), 5.72–5.96 (m, 1H), 7.10–7.64 (m, 30H). ^{13}C NMR: $\delta = 66.0$, 117.3, 128.5–135.0, 205.4. ^{31}P NMR: $\delta = 45.4$ (br). IR (CH_2Cl_2): $\nu(CO) = 2083$ (w), 2055 (vs), 2029 (w), 1999 (w), 1970 (m) cm^{-1}. MS: m/z 995 [$M^+ + H$], plus ions corresponding to sequential loss of carbonyl ligands.

4.1.4. [$Co_3(\mu_3$-CC(O)$OCH_2CH{=}CH_2)(CO)_7(PMe_3)_2$] (6)

To a toluene solution (20 mL) of **1** (0.22 g, 0.42 mmol), $Ag_4I_4(PMe_3)_4$ (0.52 g, equivalent to 0.42 mmol of PMe_3) was added. The mixture was stirred under dinitrogen whilst heating with a hot air blower. A vigorous reaction was noted with an accompanying colour change from purple to dark green. Some effervescence was also seen. Heating was continued until the evolution of gas ceased, within 1 h. Stirring was continued at room temperature overnight. The solvent was evaporated in vacuo and the residue purified by column chromatography on alumina. Using a 2:1 hexane/dichloromethane mixture as eluent a purple band (**1**) was eluted. Dichloromethane as eluent yielded a dark green band. The solvent was removed under reduced pressure from the dark green band and the residue dissolved in hexane/dichloromethane. Cooling at −10°C overnight resulted in crystallisation. The product was recrystallised from hexane giving **6**. Yield: 0.15 g, 58%. m.p.: 66–68 °C. ^{1}H NMR: $\delta = 1.42$ - 1.46 (d, 18H), 4.57–4.60 (m, 2H), 5.17–5.21 (m, 1H), 5.29–5.38 (m, 1H), 5.87–6.01 (m, 1H). ^{13}C NMR: $\delta = 19.7$ (d), 66.0, 118.3, 133.3. ^{31}P NMR: $\delta = 2.9$ (br). IR (CH_2Cl_2): ν(CO) = 2053 (s), 2000 (vs), 1962 (sh), 1950 (w), 1911 (w) cm^{-1}. MS: m/z 645 [M^+ + Na], 623 [M^+ + H], 622 [M^+].

4.1.5. [$Co_3(\mu_3$-CC(O)$OCH_2CH{=}CH_2)(CO)_6(PEt_3)_3$] (7) and [$Co_3(\mu_3$-CC(O)$OCH_2CH{=}CH_2)(CO)_7(PEt_3)_2$] (8)

Cluster **1** (0.40 g, 0.76 mmol), dichloromethane (15 mL) and triethylphosphane (0.18 mL, 1.22 mmol) were stirred at room temperature. A rapid colour change, purple to dark green, and vigorous effervescence was noted. Stirring was continued until the evolution of gas was complete (within 2 h). Solvent evaporation at reduced pressure proceeded and the residue was purified by column chromatography on silica. Using diethyl ether as eluent, a dark green band was eluted. After removal of the solvent in vacuo, the residue was dissolved in hexane (~30 mL)/dichloromethane (~0.5 mL). Evaporation of approximately a third of the solvent and cooling overnight yielded a dark green, crystalline solid **7**. Yield: 0.14 g, 23%. m.p.: 90°C. ^{1}H NMR: $\delta = 0.8$ - 1.2 (s, br), 1.5–1.9 (s, br), 4.6–4.7 (m, 2H), 5.0–5.2 (m, 1H), 5.27–5.41 (m, 1H), 5.73–5.98 (m, 1H). ^{13}C NMR: $\delta = 8.1$, 18.8 (d), 20.9 (d), 66.0, 117.4, 132.3. ^{31}P NMR: $\delta = 33.2$ (br). IR (CH_2Cl_2): ν(CO) = 2050 (m), 1998 (s), 1977 (vs), 1806 (m), 1740 (w), 1700 (vw) cm^{-1}. MS: m/z 796 [M^+].

Further, a second dark green fraction was obtained from the column using the same eluent. Evaporation of the solvent in vacuo resulted in the isolation of **8**. Yield: 50 mg, 9%. ^{1}H NMR: $\delta = 0.92$ - 1.14 (m, 6H), 1.61–1.83 (m, 4H), 4.49–4.62 (m, 2H), 5.06–5.18 (m, 1H), 5.23–5.34 (m, 1H), 5.83–5.97 (m, 1H). ^{13}C NMR: $\delta = 6.8$, 19.5 (d), 64.6, 116.5, 132.1, 181.1, 207.8. ^{31}P NMR: $\delta = 33.7$ (br). IR (CH_2Cl_2): ν(CO) = 2062 (m), 2012 (vs), 1994 (s), 1981 (w), 1975 (vw) cm^{-1}. MS: m/z 729 [M^+ + Na], 707 [M^+ + H].

4.2. X-ray crystallography for 2, 3, 5, 6 and 7

All measurements were made on a Bruker AXS SMART 1000 CCD area detector diffractometer equipped with Mo Kα radiation ($\lambda = 0.71073$ Å) at 150 K. Narrow-frame exposures (0.3° in ω) were employed. Cell parameters were refined from all strong reflections in each data set. Intensities were corrected semi-empirically for absorption, based on symmetry-equivalent and repeated reflections. The structures were solved by direct methods (Patterson synthesis for **2**) and refined by full-matrix least-squares on F^2 values for all unique data. All non-hydrogen atoms were refined anisotropically. H atoms were included in a riding model with U_{iso} set to be 1.2 times (1.5 times for methyl-H) U_{eq} for the carrier atom. In **2**, the residual electron density peaks >1 e Å^{-3} were close to Co atoms. In **3**, the PLATON 'Squeeze' procedure [35] was employed to model a half-hexane molecule which was badly disordered. 'Squeeze' recovered 48 electrons which agrees well with 50 electrons in half a hexane molecule. In the asymmetric unit of **5** there are two Co_3 clusters plus half a molecule each of CH_2Cl_2 and hexane. Restraints were applied to the anisotropic displacement parameters of the solvent molecules and to those of the capping ligand on the Co_3 cluster containing Co(1). The largest residual electron density peaks were close to the metal atoms. In **7**, a number of crystallographic problems were overcome. The crystals were twinned racemically and via a 180° rotation about b giving four twin components, three of them minor with 2%, 7% and 2% contributions. In addition, atom C(4) in the capping ligand was disordered over two sets of positions, while two and three ethyl groups on P(2) and P(3), respectively, were also disordered.

5. Supplementary material

Crystallographic data for the structural analyses have been deposited with the Cambridge Crystallographic Center, CCDC No.'s 216491–5. Copies of this information may be obtained free of charge from The Director, CCDC, 12 Union Road, Cambridge CB2 1EK (Fax: +44-1223-336033; deposit@ccdc.cam.ac.uk or www.ccdc.cam.ac.uk).

Acknowledgements

The provision of a studentship to A.E.O. by the EPSRC is gratefully acknowledged.

References

[1] B.C. Gates, Chem. Rev. 95 (1995) 511.
[2] R. Whyman, in: B.F.G. Johnson, (Ed.), Transition Metal Clusters, Wiley, 1980 (Chapter 8 and the references contained therein).
[3] G. Süss-Fink, G. Meister, Adv. Organomet. Chem. 35 (1993) 41.
[4] E.L. Muetterties, M.J. Krause, Angew. Chem., Int. Ed. Engl. 22 (1983) 135.
[5] R.C. Ryan, C.U. Pittman Jr., J.P. O'Connor, J. Am. Chem. Soc. 99 (1977) 1986.
[6] D. Seyferth, H.P. Withers, Inorg. Chem. 22 (1983) 2931.
[7] J. Collin, C. Jossart, G. Balavoine, Organometallics 5 (1986) 203.
[8] G. Balavoine, J. Collin, J.J. Bonnet, G. Lavigne, J. Organomet. Chem. 280 (1985) 429.
[9] M. Castiglioni, R. Giordano, E. Sappa, J. Organomet. Chem. 342 (1988) 111.
[10] A. Fumagalli, T.F. Koetzle, F. Takusagawa, P. Chini, S. Martinengo, B.T. Heaton, J. Am. Chem. Soc. 102 (1980) 1740.
[11] R.B. King, A.D. King Jr., K. Tanaka, J. Mol. Catal. 10 (1980) 75.
[12] H.Y. Chien, M.G. Richmond, K.Y. Yang, J. Mol. Catal. 88 (1994) 159.
[13] (a) D. Seyferth, A.T. Wehman, J. Am. Chem. Soc. 92 (1970) 5520;
(b) D. Seyferth, J.E. Hallgren, R.J. Spohn, J. Organomet. Chem. 23 (1970) C55;
(c) D. Seyferth, P.L.K. Hung, J.E. Hallgren, J. Organomet. Chem. 44 (1972) C55.
[14] D. Seyferth, G.H. Williams, C.L. Nivert, Inorg. Chem. 16 (1977) 758.
[15] B.F.G. Johnson, A.J. Blake, A.J. Brown, S. Parsons, P. Taylor, J. Chem. Soc., Chem. Commun. (1995) 117.
[16] D. Seyferth, G.H. Williams, C.L. Nivert, Inorg. Synth. 20 (1980) 234.
[17] A.J. Downard, B.H. Robinson, J. Simpson, Organometallics 5 (1986) 1122.
[18] M.J. Don, M.G. Richmond, W.H. Watson, M. Krawiec, R.P. Kashyap, J. Organomet. Chem. 418 (1991) 231.
[19] K. Yang, S.G. Bott, M.G. Richmond, J. Organomet. Chem. 454 (1993) 273.
[20] A.J. Downard, B.H. Robinson, J. Simpson, J. Organomet. Chem. 447 (1993) 281.
[21] D.N. Duffy, M.M. Kassis, A.D. Rae, Acta Crystallogr., Sect. C 47 (1991) 2054.
[22] (a) S.O. Grim, L.C. Satek, C.A. Tolman, J.P. Jesson, Inorg. Chem. 14 (1975) 656;
(b) V.V. Grushin, J. Am. Chem. Soc. 121 (1999) 5831.
[23] S. Bittner, M. Pomerantz, Y. Assaf, P. Krief, S. Xi, M.K. Witczak, J. Org. Chem. 53 (1988) 1.
[24] S. Aime, M. Botta, R. Gobetto, D. Osella, J. Organomet. Chem. 320 (1987) 229.
[25] S.G. Bott, J.C. Wang, M.G. Richmond, J. Chem. Crystallogr. 29 (1999) 603.
[26] K. Hinkelmann, J. Heinze, H.-T. Schacht, J.S. Field, H. Vahrenkamp, J. Am. Chem. Soc. 111 (1989) 5078.
[27] Y.-P. Wang, Z.-Q. Lei, H.-Y. Feng, Y.-H. Liu, Appl. Organomet. Chem. 5 (1991) 517.
[28] M.D. Brice, B.R. Penfold, W.T. Robinson, S.R. Taylor, Inorg. Chem. 9 (1970) 362.
[29] T.W. Matheson, B.H. Robinson, W.S. Tham, J. Chem. Soc. A (1971) 1457.
[30] A.J. Downard, B.H. Robinson, J. Simpson, Organometallics 5 (1986) 1132.
[31] P.A. Dawson, B.H. Robinson, J. Simpson, J. Chem. Soc., Dalton Trans. (1979) 1762.
[32] J. Evans, B.F.G. Johnson, J.R. Norton, F.A. Cotton, J. Chem. Soc., Chem. Commun. (1973) 807.
[33] T.W. Matheson, B.H. Robinson, J. Organomet. Chem. 88 (1975) 367.
[34] C.A. Tolman, Chem. Rev. 77 (1977) 313.
[35] A.L. Spek, Acta Crystallgr., Sect. A 46 (1990) C34.